# Asymptotic description of fluid flows

Edgar Knobloch

Department of Physics
University of California, Berkeley, CA 94720, USA

knobloch@berkeley.edu

http://tardis.berkeley.edu

with Keith Julien, University of Colorado, and many others

Staircase-21, KITP, 28 January 2021

## Rotationally Constrained Convection
## $Ra$–$Ta$ Parameter Space: Experiments

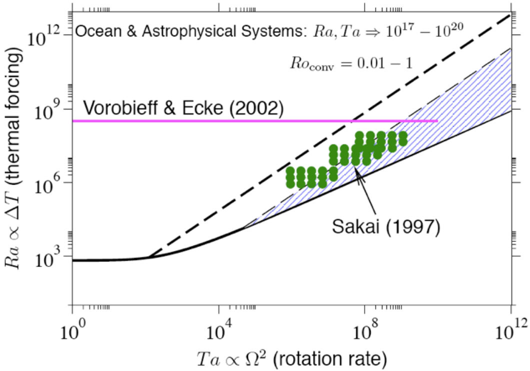


NHBGE captures large Ta - low Ro regime for Rayleigh-Benard convection

Sunday, September 30, 12

# Asymptotic reduction of the primitive equations

$$\mathbf{u}_t + \mathbf{u}\cdot\nabla\mathbf{u} + \frac{1}{Ro}\hat{\mathbf{z}}\times\mathbf{u} = -P\nabla p + \Gamma T\hat{\mathbf{z}} + \frac{1}{Re}\nabla^2\mathbf{u}$$

$$T_t + \mathbf{u}\cdot\nabla T = \frac{1}{Pe}\nabla^2 T$$

$$\nabla\cdot\mathbf{u} = 0,$$

where

$$Ro = \frac{U}{2\Omega L}, \quad P = \frac{\tilde{P}}{\rho_0 U^2}, \quad Re = \frac{UL}{\nu}, \quad Pe = \frac{UL}{\kappa}, \quad \Gamma = -\frac{g\alpha\tilde{T}L}{U^2}$$

and $L$ and $U$ are arbitrary horizontal length and velocity scales to be selected depending on the process of interest. We suppose that $Ro \equiv \epsilon \ll 1$ and $H/L = \epsilon^{-1}$ with

$$\partial_x \to \epsilon^{-1}\partial_x, \quad \partial_y \to \epsilon^{-1}\partial_y, \quad \partial_z \to \partial_Z, \quad \partial_t \to \epsilon^{-2}\partial_t + \partial_\tau.$$

The slow spatial scale $Z$ is required by the boundary conditions.

# Asymptotic reduction of the primitive equations

An asymptotic expansion in $\epsilon$ with $u \sim v \sim W = \mathcal{O}(1)$, $T = \overline{T} + \epsilon\theta$, and $\Gamma = \mathcal{O}(\epsilon^{-1})$, $P = \mathcal{O}(\epsilon^{-1})$, leads at $\mathcal{O}(\epsilon^{-1})$ to **geostrophic balance**:

$$\hat{\mathbf{z}} \times \mathbf{u}_\perp = -\nabla_\perp p, \quad \nabla_\perp \cdot \mathbf{u}_\perp = 0, \quad \mathbf{u}_\perp = (-\psi_y, \psi_x), \quad \psi \equiv p.$$

At $\mathcal{O}(1)$ the vertical vorticity $\omega \equiv \nabla_\perp^2 \psi$ and vertical velocity $W$ satisfy

$$\partial_t \omega + J[\psi, \omega] - \partial_Z W = Re^{-1} \nabla_\perp^2 \omega$$

$$\partial_t W + J[\psi, W] + \partial_Z \psi = \Gamma\theta + Re^{-1} \nabla_\perp^2 W.$$

Fluctuating buoyancy equation at $\mathcal{O}(\epsilon^1)$:

$$\partial_t \theta + J[\psi, \theta] + W \partial_Z \overline{T} = Pe^{-1} \nabla_\perp^2 \theta.$$

Mean buoyancy equation at $\mathcal{O}(\epsilon^1)$:

$$\partial_\tau \overline{T} + \partial_Z \overline{W\theta} = Pe^{-1} \partial_{ZZ} \overline{T}.$$

# Summary of the reduced model

With the choice $L/H = E^{1/3}$ ($E = \nu/2\Omega H^2$) and $U = \nu/L$ the resulting system is

$$\partial_t \omega + J[\psi, \omega] - \partial_Z W = \nabla_\perp^2 \omega + O(E^{1/3})$$
$$\partial_t W + J[\psi, W] + \partial_Z \psi = \sigma^{-1} Ra E^{4/3} \theta + \nabla_\perp^2 W + O(E^{1/3})$$
$$\partial_t \theta + J[\psi, \theta] + W \partial_Z \overline{T} = \sigma^{-1} \nabla_\perp^2 \theta + O(E^{1/3})$$
$$\partial_\tau \overline{T} + \partial_Z \overline{W\theta} = \sigma^{-1} \partial_{ZZ} \overline{T} + O(E^{1/3}),$$

where $Ra$ is the Rayleigh number and $\sigma \equiv \nu/\kappa$ is the Prandtl number; we assume that $RaE^{4/3} = O(1)$, $\sigma = O(1)$. These equations are to be solved subject to the boundary conditions

$$W = \psi_Z = \theta = 0, \quad \overline{T} = 1, \quad \text{on} \quad Z = 0,$$
$$W = \psi_Z = \theta = 0, \quad \overline{T} = 0, \quad \text{on} \quad Z = 1,$$

and PBC in the horizontal. The overbar denotes horizontal average, followed by an average over fast time, and $J(f, g) \equiv f_x g_y - f_y g_x$. The equations constitute a **closed reduced system** referred to as NHBGE (nonhydrostatic balanced geostrophic equations).

# What have we achieved?

The nonhydrostatic balanced geostrophic equations (NHBGE)

- eliminate thin Ekman boundary layers; thermal layers remain
- filter out fast inertial waves; moreover, on the scales of interest the inviscid dispersion relation for modes $\propto \exp i(\lambda t + \mathbf{k}_\perp \cdot \mathbf{x}_\perp + k_z Z)$ is

$$\lambda^2_{\text{reduced}} = \frac{k_z^2}{k_\perp^2}, \qquad \text{cf.} \quad \lambda^2_{\text{NS}} = \frac{k_z^2}{k_\perp^2 + E^{2/3} k_z^2}$$

These facts allow us to integrate the NHBGE with less resolution and much larger time step than have to be used when solving the primitive equations. **Note** that the resulting equations

- describe asymptotically precisely the fluid problem even though they do not look like NSE
- are fully three-dimensional
- are fully nonlinear
- moreover, they are $D_4 \dot{+} T^2$-symmetric, i.e., there is no handedness to the flow at leading order. Thus as $E \to 0$ the numbers of cyclonic and anticyclonic vortices should become **equal**.

# Exact single mode solutions

The reduced equations have exact (but unstable) steady solutions of the form $(\psi, W, \theta) = \mathrm{Re}(\sigma^{-1} A(Z), \sigma^{-1} B(Z), C(Z)) \exp ik_\perp x$, where

$$\frac{d^2 B}{dZ^2} - k_\perp^2 Nu Ra E^{4/3} \left(1 + \frac{1}{2k_\perp^2}|B|^2\right)^{-1} B = 0; \; Nu^{-1} = \int_0^1 (1 + \frac{1}{2k_\perp^2}|B|^2)^{-1} dZ$$

This is a nonlinear eigenvalue problem for the Nusselt number $Nu$ given $RaE^{4/3}$ which can be used to generate highly nonlinear states:

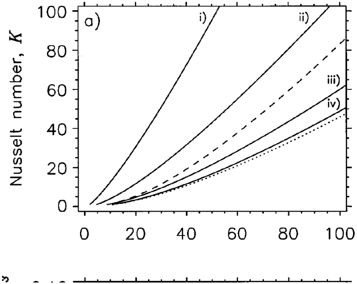


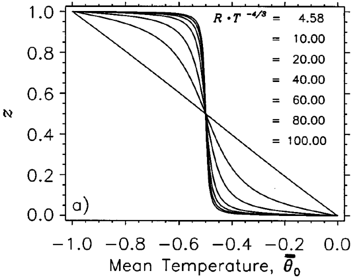

# Regimes described by the reduced system

The reduced equations describe four distinct dynamical regimes, depending on the values of the Rayleigh number $Ra \equiv g\alpha\Delta TH^3/\nu\kappa$ and the Prandtl number $\sigma \equiv \nu/\kappa$:

- Cellular convection (C)
- Convective Taylor columns (T)
- Convective plumes (P)
- Geostrophic turbulence (G)

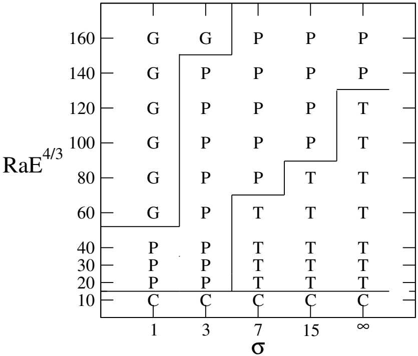

# Regimes described by the reduced system

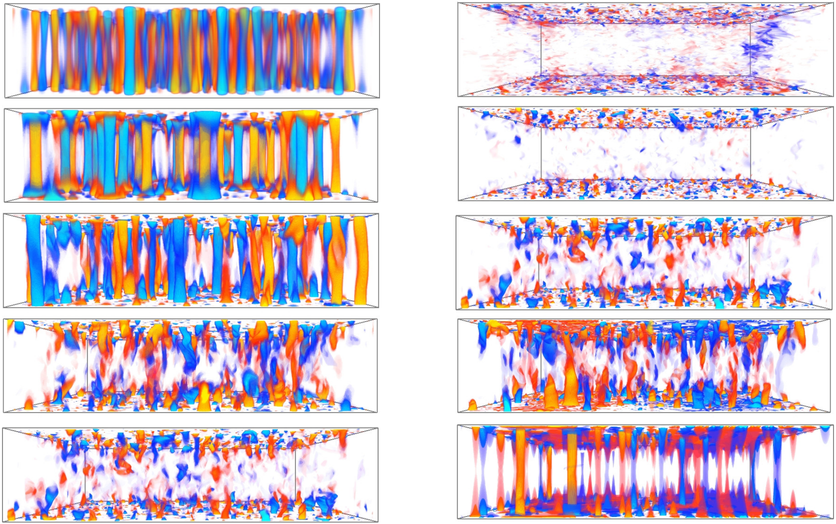

Volume renders of $\theta$ for $RaE^{4/3} = 20, 40, 80, 120, 160$ and $\sigma = 7$ (left) and $RaE^{4/3} = 160$ and $\sigma = 1, 3, 7, 15, \infty$ (right)

# Evolution of barotropic mode

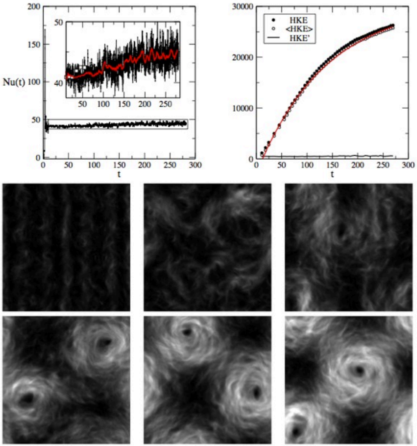


Sunday, September 30, 12

Julien et al., GAFD **106**, 392–428 (2012): $Ra\, E^{4/3} = 100$, $\sigma = 1$

# Spontaneous formation of large scale vortices

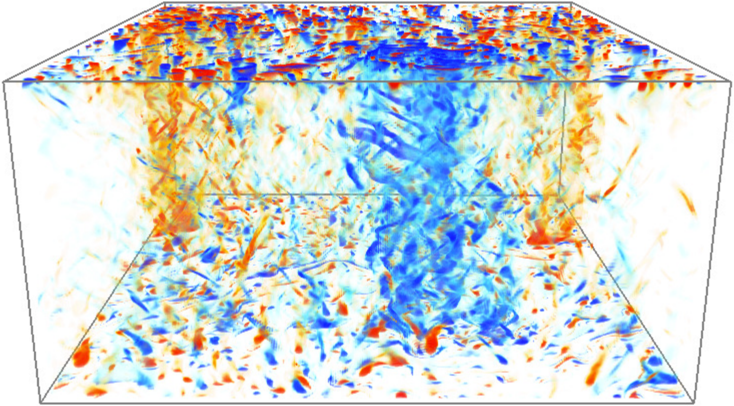

Rubio et al., PRL **112**, 144501 (2014): $Ra\,E^{4/3} = 100$, $\sigma = 1$

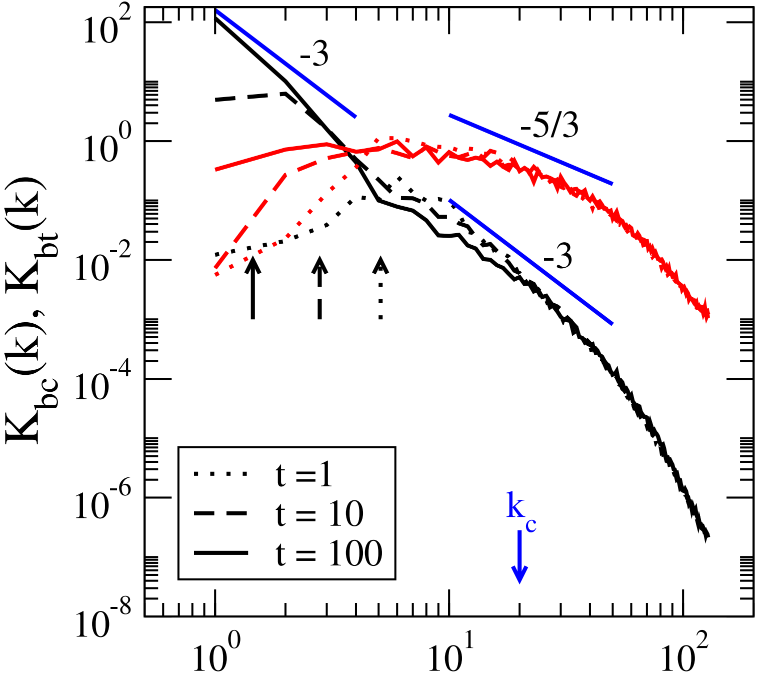

$K_{bc}(k), K_{bt}(k)$
$10^{2}$
$10^{0}$
$10^{-2}$
$10^{-4}$
$10^{-6}$
$10^{-8}$
$10^{0}$
$10^{1}$
$10^{2}$
-3
-5/3
-3
t =1
t = 10
t = 100
$k_c$

# Barotropic/baroclinic vorticity equations

Let $\omega = \langle\omega\rangle + \omega'$, $\psi = \langle\psi\rangle + \psi'$, where $\langle \dots \rangle$ denotes a depth average.

Then

$$\langle\omega\rangle_t + J[\langle\psi\rangle, \langle\omega\rangle] + \langle J[\psi', \omega']\rangle = \nabla_\perp^2 \langle\omega\rangle$$

and

$$\omega'_t + J[\langle\psi\rangle, \omega'] + J[\psi', \langle\omega\rangle] + J[\psi', \omega']' - DW = \nabla_\perp^2 \omega'.$$

Thus the baroclinic-baroclinic term acts as a source term for the barotropic mode. Without this term the barotropic flow is identical to 2D hydrodynamics and an inverse energy cascade to large scales is expected. In fact this is so even in the presence of this term, and leads to a $k_\perp^{-3}$ pile up at large scales, eg., Smith and Waleffe, Phys. Fluids **11**, 1608 (1999).

However, the fluctuation equation is fully 3D and hence exhibits the usual $k_\perp^{-5/3}$ energy spectrum expected from Kolmogorov theory.

The emergence of a coherent structure from a turbulent state has been termed spectral **condensation** [PRL **95**, 263901 (2005); **101**, 194504 (2008); **112**, 144501 (2014), cf H Xia, M Shats, G Falkovich, A Frishman]

# Time evolution of baroclinic and barotropic modes

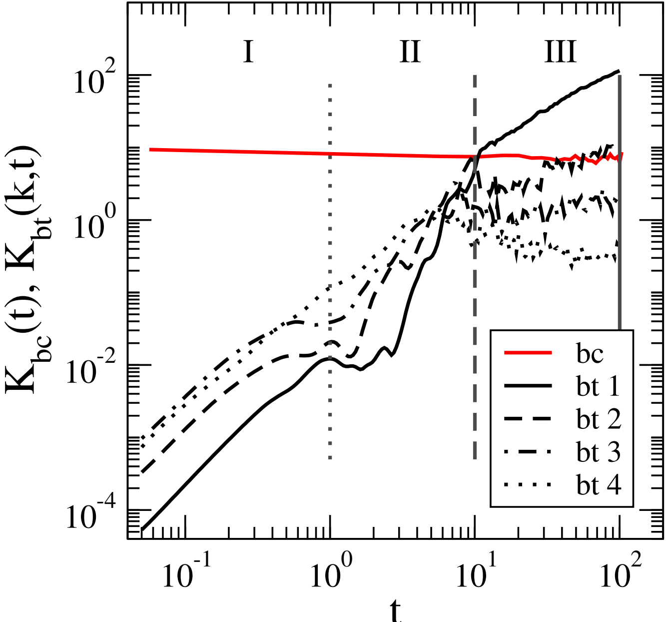

# Validation: $E = 10^{-7}$ (Stellmach 2012, unpublished)

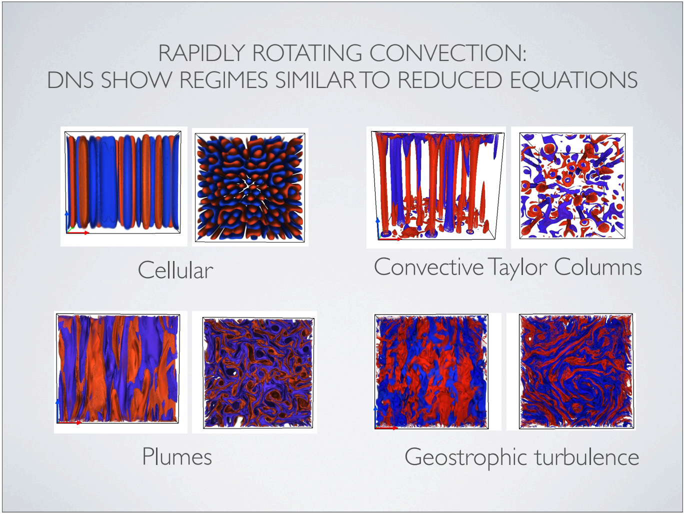


Cellular regime: $\sigma = 1$, $Ra\,E^{4/3} = 11$; CTC regime: $\sigma = 15$, $Ra\,E^{4/3} = 15$; Plume regime: $\sigma = 3$, $Ra\,E^{4/3} = 50$; GT regime: $\sigma = 1$, $Ra\,E^{4/3} = 90$

# Validation (ctd)

The primitive equations have to be solved at finite Ekman number:

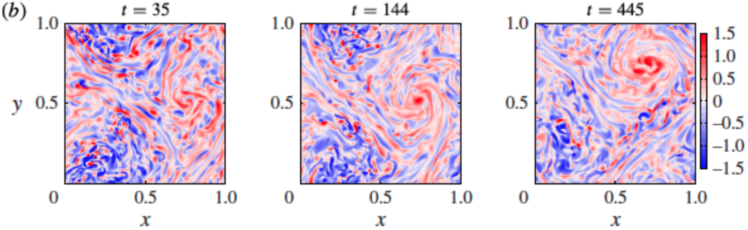


FIGURE 9. (Colour online) (*a*) Time evolution of the r.m.s. velocity after an inversion of the sign of the vorticity at $t = 0$. (*b*) Horizontal cross-sections (at $z = 0.25$) of the axial vorticity at different times, indicated by the vertical lines in (*a*). The simulation was initialised at the time shown in figure 2(*a*), with the same input parameters, but with vorticity of the opposite sign (series S5, $\widetilde{Ra} = 68$).

Guervilly, Hughes & Jones, JFM **758**, 407 (2014): $E = 5 \times 10^{-6}$, $Ra\, E^{4/3} = 68$, $\sigma = 1$

# Validation (ctd)

The primitive equations have to be solved at finite Ekman number:

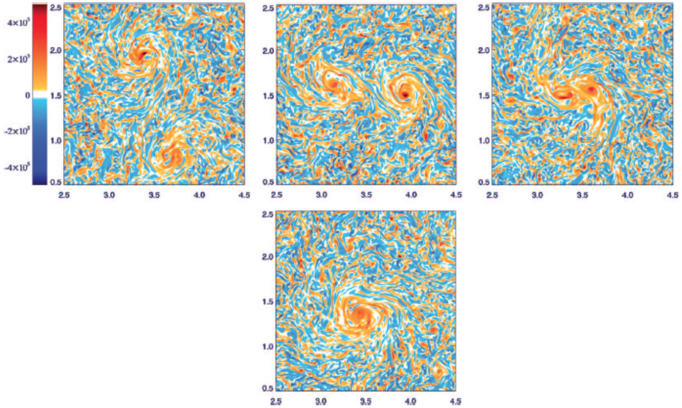

Favier, Silvers & Proctor, PF **26**, 096605 (2014): $E = 10^{-5}$, $Ra\, E^{4/3} = 107.7$, $\sigma = 1$

# Validation (ctd)

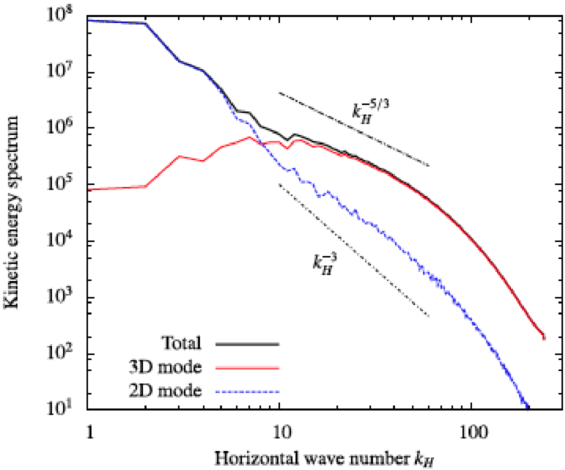


Favier, Silvers & Proctor, PF **26**, 096605 (2014): $E = 10^{-5}$, $Ra\,E^{4/3} = 107.7$, $\sigma = 1$

# Validation (ctd)

The primitive equations have to be solved at finite Ekman number:

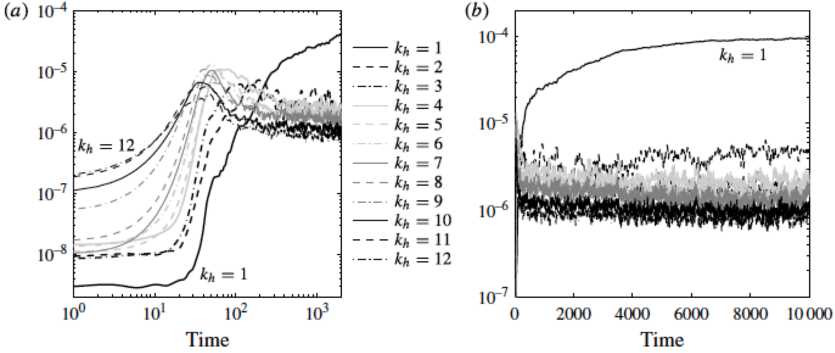


Guervilly, Hughes & Jones, JFM **758**, 407 (2014): $E = 5 \times 10^{-6}$, $Ra\, E^{4/3} = 34$, $\sigma = 1$

# Effect of horizontal aspect ratio: jet formation

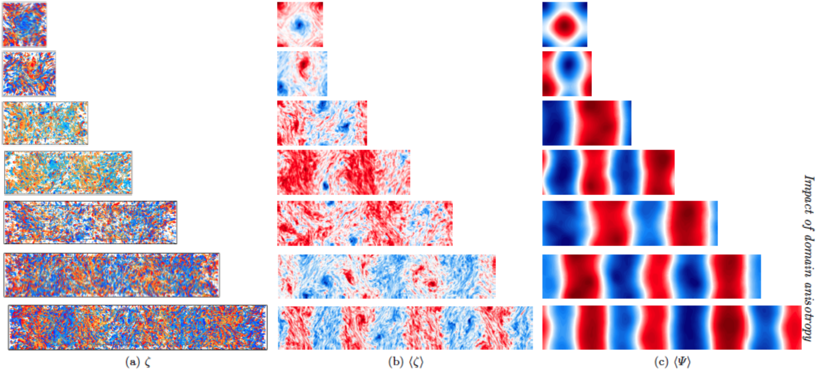


Parameters: $Ra\,E^{4/3} = 90$, $\sigma = 1$; aspect ratios $A = 1, 1.1, 2, 3, 4, 5$ and $6$

Julien et al., JFM **837**, R4 (2018)

# Validation

The primitive equations have to be solved at finite (and finite) Ekman number:

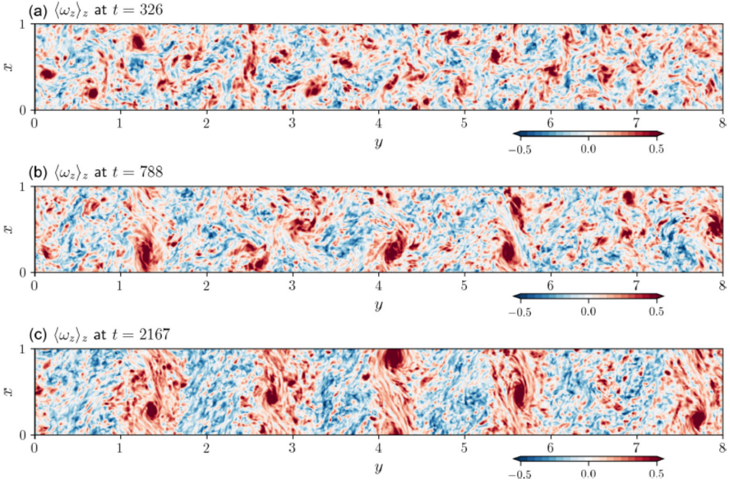


Guervilly & Hughes, PRF **2**, 113503 (2017): $E = 10^{-5}$, $Ra\, E^{4/3} = 62$

# Salt-finger turbulence in two dimensions

The nondimensional equations for fluctuations around the conduction state $\psi = 0$, $T_{\rm total} = S_{\rm total} = z$ are

$$\frac{\tau}{\sigma}\left[\frac{\partial}{\partial t}\nabla^2\psi + J(\psi, \nabla^2\psi)\right] = \frac{1}{\tau}\frac{\partial \tilde{T}}{\partial x} - \frac{1}{\tau R_\rho}\frac{\partial \tilde{S}}{\partial x} + \nabla^4\psi,$$

$$\frac{\partial}{\partial t}\tilde{T} + J(\psi, \tilde{T}) + \frac{\partial \psi}{\partial x} = \tau^{-1}\nabla^2\tilde{T},$$

$$\frac{\partial}{\partial t}\tilde{S} + J(\psi, \tilde{S}) + \frac{\partial \psi}{\partial x} = \nabla^2\tilde{S}.$$

The three dimensionless ratios are the Prandtl number $\sigma$, the inverse Lewis number $\tau$ and the density ratio $R_\rho$ specifying the contribution of $T$ and $S$ to the background density gradient. A fourth dimensionless ratio, the Schmidt number $\mathrm{Sc}$, is also important:

$$\sigma = \frac{\nu}{\kappa_T}, \qquad \tau = \frac{\kappa_S}{\kappa_T}, \qquad \mathrm{Sc} = \frac{\nu}{\kappa_S}, \qquad R_\rho = \frac{\alpha_T\beta_T}{\alpha_S\beta_S}\,.$$

We adopt doubly periodic boundary conditions for $\psi$, $\tilde{T}$ and $\tilde{S}$, and focus on the salt-finger regime $1 < R_\rho < \tau^{-1}$.

# The regime $\tau \ll 1$

We consider two cases, distinguished by the magnitude of the Schmidt number $\mathrm{Sc}$. For $\mathrm{Sc} = O(1)$, i.e. $\kappa_S \sim \nu$, we obtain the small Prandtl number regime $\sigma = O(\tau)$ of astrophysical relevance. This results in a modified Rayleigh-Bénard convection (MRBC) system with salinity-driven instability and rapidly diffusing temperature. The large Schmidt number regim, i.e. $\kappa_S \ll \nu$ (equivalently $\tau \ll \sigma$), is relevant for oceanic thermohaline flows where $\mathrm{Sc} \approx 700$ and $\tau \approx 0.01$. This results in a model where inertial forces are small and salinity is the only slowly diffusing quantity, leading to the inertia-free salt convection (IFSC) model.

In all cases we suppose that the density ratio $R_\rho$ is large and comparable to $\tau^{-1}$. This is a reasonable assumption for many geophysical and astrophysical applications. We therefore define the $O(1)$ parameter

$$\mathrm{Ra} \equiv \frac{1}{R_\rho \tau} = \frac{\mathrm{Ra}_S}{\mathrm{Ra}_T}$$

and refer to $\mathrm{Ra}$ as the Rayleigh ratio.

# The MRBC and IFSC models

With

$$T_{\text{total}} = z + \tau\, T\,, \qquad S_{\text{total}} = z + \mathrm{Ra}^{-1}\, S$$

and $\mathrm{Sc} = O(1)$ ($\kappa_S \sim \nu$) we obtain the **MRBC model**:

$$\frac{1}{\mathrm{Sc}}\left[\frac{\partial}{\partial t}\nabla^2\psi + J(\psi, \nabla^2\psi)\right] = -\frac{\partial S}{\partial x} + \left(\nabla^4 + \Delta^{-1}\partial_x^2\right)\psi\,,$$

$$\frac{\partial}{\partial t}S + J(\psi, S) + \mathrm{Ra}\frac{\partial\psi}{\partial x} = \nabla^2 S.$$

Here the inverse Laplacian comes from solving

$$\frac{\partial\psi}{\partial x} = \nabla^2 T\,.$$

With $\mathrm{Sc} \gg 1$ ($\kappa_S \ll \nu$) we obtain instead the **IFSC model**:

$$\left(\partial_x^2 + \nabla^6\right)\psi = \partial_x\nabla^2 S\,,$$

$$\frac{\partial}{\partial t}S + J(\psi, S) + \mathrm{Ra}\frac{\partial\psi}{\partial x} = \nabla^2 S.$$

These reduced equations are solved in doubly periodic domains.

# The IFSC model

The model has growing finger solutions: $(\psi, S) = (\psi_0, S_0)\exp\{\lambda t + ikx\}$. These are **exact** nonlinear solutions in the presence of PBC in $(x, z)$.

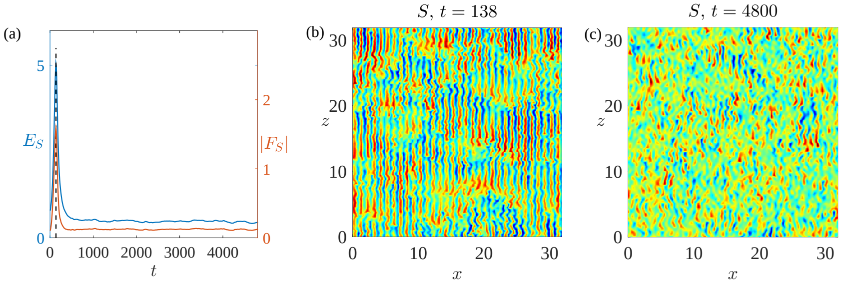


Results from a $32\ell_{\rm opt} \times 32\ell_{\rm opt}$ simulation for $\mathrm{Ra} = 1.1$. (a) Evolution of the total energy $E_S$ and the salinity flux $|F_S|$ with time. The dashed line marks $t = 138$, where both quantities peak. (b) The finger-dominated state at $t = 138$. (c) The instantaneous statistically steady state at $t = 4800$, the end of this simulation. Distances are measured in units of $\ell_{\rm opt}$, the wavelength of the optimal mode.

# IFSC: Turbulent salt-finger convection

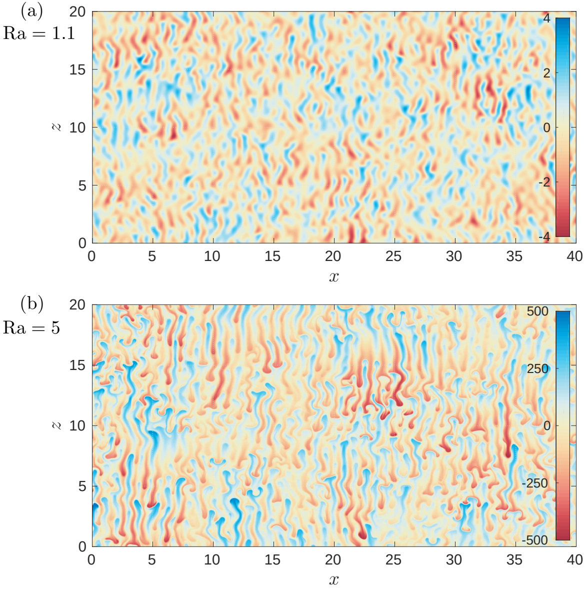

# The MRBC model: $\mathrm{Ra} = 2$, $\mathrm{Sc} = 1$

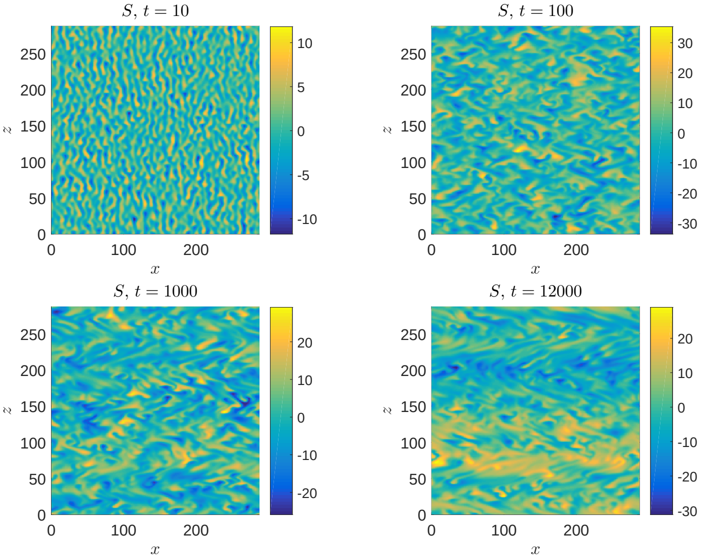


Snapshots of $S(x, z, t)$ at $t = 10$, $100$, $1000$ and $12000$

# The MRBC model: $\mathrm{Ra} = 2$, $\mathrm{Sc} = 1$

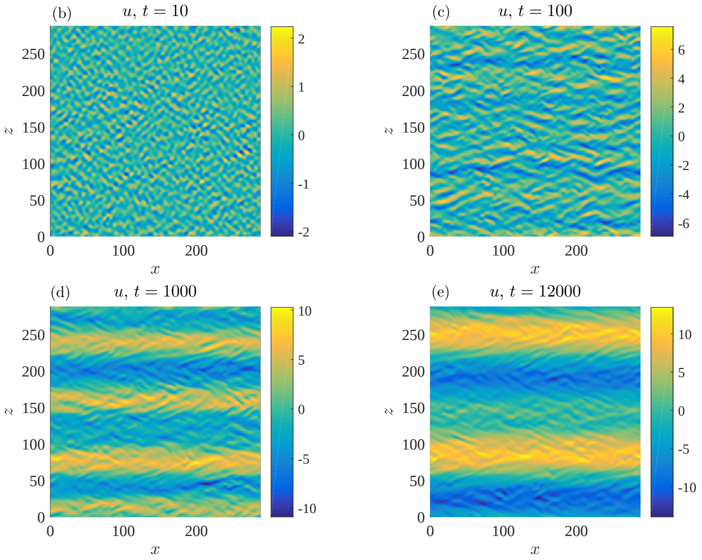


Snapshots of $u(x, z, t)$ at $t = 10, 100, 1000$ and $12000$

# The MRBC model: $\mathrm{Ra} = 2$ and $\mathrm{Sc} = 1$

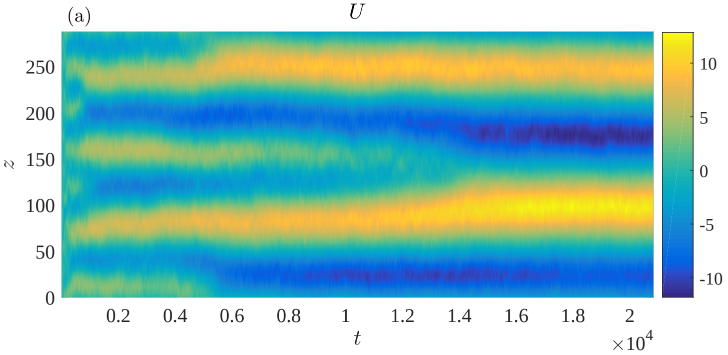


Space-time evolution of the jet profile $\bar{U}(z,t)$ in the MRBC system when $\mathrm{Ra} = 2$ and $\mathrm{Sc} = 1$

# The MRBC model: $\mathrm{Ra} = 2$ and $\mathrm{Sc} = 1$

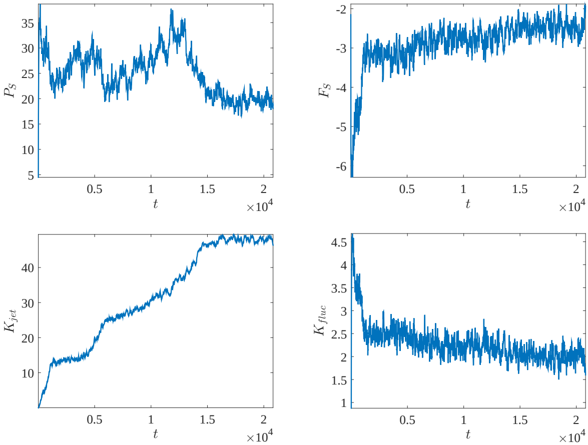


Evolution of salinity potential energy $P_S$, salinity flux $F_S$, kinetic energy $K_{jet}$ in the jets and the fluctuation kinetic energy $K_{fluc}$ in a doubly periodic domain of size $L_x \times L_z = 32 l_{\mathrm{opt}} \times 32 l_{\mathrm{opt}}$ obtained from the MRBC equations when $\mathrm{Ra} = 2$ and $\mathrm{Sc} = 1$. A statistically stationary state is present for $t \gtrsim 1.5 \times 10^4$.

# Advantages of the asymptotic approach:

- The reduced equations are asymptotically exact as $E \to 0$, $Ra\, E^{4/3} = \mathcal{O}(1)$
- The reduced equations permit study of regimes relevant to geophysical and astrophysical flows
- The equations contain no small or large parameters
- The equations capture, apparently correctly, the physics of RRRBC, including Taylor columns, plumes and geostrophic turbulence
- They capture the formation of large scale structure: domain-size vortices and jets
- Equations offer opportunity to study fundamental properties of $2+\epsilon$-dimensional flows

**Disadvantages of the asymptotic approach:**

- The equations focus on one particular regime: $L/H = \mathcal{O}(\mathrm{Ro})$ and may not describe other regimes
- Applications always require finite $E$: when are the dynamics at a given $E$ captured by the reduced equations?
- The equations only represent slow dynamics; no inertial wave turbulence
- Ekman pumping is absent; may be added as subdominant boundary forcing

# Future:

- What is special about $L/H = \mathcal{O}(\mathrm{Ro})$ that allows closure?
- Are there other regimes where closure is possible?
- The approach points to the importance of phases of the small scales: can this be confirmed and the interaction between the large scales and the phases of the small scales be understood?
- Is homogeneous anisotropic turbulence in some sense (which?) unstable to the formation of large scale structure?
- Is this a subcritical bifurcation? Or are the large scale structures noise-sustained?
- Can a similar description of the fast dynamics be developed and the two descriptions coupled?
- Can vortices be computed as localized structures of the NHBGE?
- Can their stability properties be determined and interactions among them studied?

The approach generalizes to other systems with strong restraints, including salt-finger convection, magnetoconvection, magnetorotational instability, Langmuir circulation, shear flows, stratified flows, GSF instability etc.

# References

Keith Julien and I have written a general description and discussion of asymptotic reduction for fluid systems with strong restraints:

K Julien, E Knobloch, J Math Phys **48**, 065405 (2007)

Rotating convection:

K Julien, E Knobloch and J Werne, Th. Comp. Fl. Dyn. **11**, 251–261 (1998)
M Sprague, K Julien, E Knobloch and J Werne, JFM **551**, 141–174 (2006)
K Julien, E Knobloch, R Milliff and J Werne, JFM **555**, 233–274 (2006)
I Grooms, K Julien, JB Weiss and E Knobloch, PRL **104**, 224501 (2010)
K Julien, AM Rubio, I Grooms and E Knobloch, GAFD **106**, 392–428 (2012)
K Julien, E Knobloch, AM Rubio and GM Vasil, PRL **109**, 254503 (2012)
AM Rubio, K Julien, E Knobloch and JB Weiss, PRL **112**, 144501 (2014)
K Julien, JM Aurnou, MA Calkins, E Knobloch et al., JFM **798**, 50–87 (2016)
K Julien, E Knobloch and M Plumley, JFM **837**, R4 (2018)
B Favier, C Guervilly and E Knobloch, JFM **864**, R1 (2019)

Salt-finger turbulence:

J-H Xie, B Miquel, K Julien and E Knobloch, Fluids **2**, 6:1–26 (2017)
J-H Xie, K Julien and E Knobloch, JFM **858**, 228–263 (2019)